

Aerodynamic Performance of a Single-stage Transonic Axial Compressor using Recirculation-Bleeding Channels

Tien-Dung Vuong¹, Duc-Manh Dinh¹, Cong-Truong Dinh^{1*}, Xuan-Long Bui²

¹ Hanoi University of Science and Technology – No. 1, Dai Co Viet Str., Hai Ba Trung, Ha Noi, Viet Nam

² Viettel Aerospace Institute – Hoa Lac, Ha Noi

Received: August 10, 2018; Accepted: November 28, 2019

Abstract

This paper investigates the recirculation channel with an addition of bleeding channels located on shroud surface of recirculation channel in the rotor domain, where the bleeding system consists of 36 channels distributed on the recirculation channel. This study focuses on its effects on aerodynamic performance of a single-stage transonic axial compressor, NASA Stage 37. Validation of numerical results was performed using experimental data for a single-stage transonic axial compressor. A parametric study with only three position of the bleeding channels were performed in a single-stage transonic axial compressor, NASA Stage 37. The numerical results showed the aerodynamic performance of a single-stage transonic axial compressor was increased, such as total pressure ratio, adiabatic efficiency, stall margin as compared to the smooth casing.

C_r Keywords: Single-stage transonic axial compressor, Recirculation-bleeding channels, Reynolds-averaged Navier-Stokes analysis, Total pressure ratio, Adiabatic efficiency, Stall margin.

Nomenclature

Notation

	chord length of blade tip (mm)
L_I	distance from rotor injection and rotor leading edge (mm)
L_E	distance from rotor ejection and rotor leading edge (mm)
\dot{m}_{peak}	mass flow rate at peak efficiency condition (kg/s)
\dot{m}_{stall}	mass flow rate at near-stall condition (kg/s)
P_t	total pressure (Pa)
T_t	total temperature ($^{\circ}$ C)

Greek symbols

α	injection angle of rotor bleeding ejector ($^{\circ}$)
β	ejection angle of rotor bleeding ejector ($^{\circ}$)
ϕ	coverage angle of rotor bleeding ejector ($^{\circ}$)
γ	specific heat ratio
η	adiabatic efficiency (%)

Abbreviations

CFD	computational fluid dynamics
EFF	adiabatic efficiency (%)
LSZ	low speed zone
PR	total pressure ratio
RANS	Reynolds-averaged Navier-Stokes
SM	stall margin (%)
SRE	stable range extension (%)

Subscripts

max	choking mass flow point
peak	peak adiabatic efficiency point
stall	near-stall point
in	inlet
out	outlet

1. Introduction

Flow through tip clearance of an axial compressor is an important element affecting the inception of stall and surge, and thus is a key concern in researches to improve the stability of the compressor. The tip clearance behavior is complex, which involves the interactions of leakage flow, end-wall boundary and blade wakes. An early experimental study from Hunter and Cumpsty [1] revealed some aspects of the flow in tip clearance region as well as the important role of tip clearance on compressor's performance.

Recirculation casing treatment is one method that shows much potential in enhancing compressor performance and stability by dealing with undesirable phenomena in the tip clearance region. Koff et al [2], Hobbs [3], and Nolcheff [4] investigated a circumferential recirculation from the rear near the trailing edge to the front near the leading edge of a rotor blade on an axial compressor's shroud surface. Air is bled from the region with highest pressure, then re-injected to the upstream location to energize the low momentum fluid, thus extend the operating range of the compressor. Hathaway [5] suggested a self-recirculating casing treatment concept which

* Corresponding author: Tel.: (+84) 934.638.035
Email: truong.dinhcong@hust.edu.vn

provided an increase in stall margin, pressure rise as well as compressor's efficiency by combining tip injection and bleeding. Strazisar et al. [6] presented end-wall recirculation stall control with airflow being bled from a casing downstream of a stator blade row and then re-injected as a wall jet upstream of a preceding rotor row. The result was an extension of the stable operating range of high-speed, highly loaded compressor. Recently, Dinh et al. [7] investigated a feed-back channel to enhance operating stability of a single stage compressor. The result was an increase of 26.8% in stall margin with only 0.14% decrease in efficiency.

The present work investigates the bleeding channels on the feed-back channel with two parts: the recirculation channel and sub-bleeding channels. Through the recirculation channel, high pressure air was extracted from the downstream and re-injected to the upstream location between the trailing and leading edges of rotor blades. With the addition of sub-bleeding channels, the feed-back channel could also perform bleed air extraction. Low momentum air would still be removed from the tip clearance region as in recirculation but would be bleed outside instead of being re-injected upstream. A parametric study was performed using geometric parameters of the sub-bleeding channels using three-dimensional (3D) Reynolds-averages Navier-Stokes (RANS) equations to find their effects on the performance of a single-stage axial compressor (NASA Stage 37).

2. Numerical Analysis

2.1. Description of Geometry

The single-stage transonic axial compressor investigated in this research by Reid and Moore [8] was NASA Stage 37 with 36 blades of Rotor 37 at a rotation speed of 17185.7 rpm (100% of design speed) and 46 blades of Stator 37. The values of the tip clearance for rotor and stator blades of this single-stage compressor were 0.04 cm under the rotor shroud and 0.0762 cm over the stator hub, respectively. The peak adiabatic efficiency and total pressure ratio at peak adiabatic efficiency were 84.00% and 2.00, respectively, at a mass flow rate of 20.74 kg/s (peak efficiency condition). The choking mass flow rate was 20.93 kg/s at 100% of design speed, and the reference temperature and pressure were 288.15 K and 101,325 Pa, respectively.

The geometry of the single-stage compressor and the recirculation-bleeding channels was generated using ANSYS 19.1 [9] as shown in Fig. 1, where the rotor and stator domains were created by using BladeGen and the recirculation-bleeding channels were built by using Design Modeler.

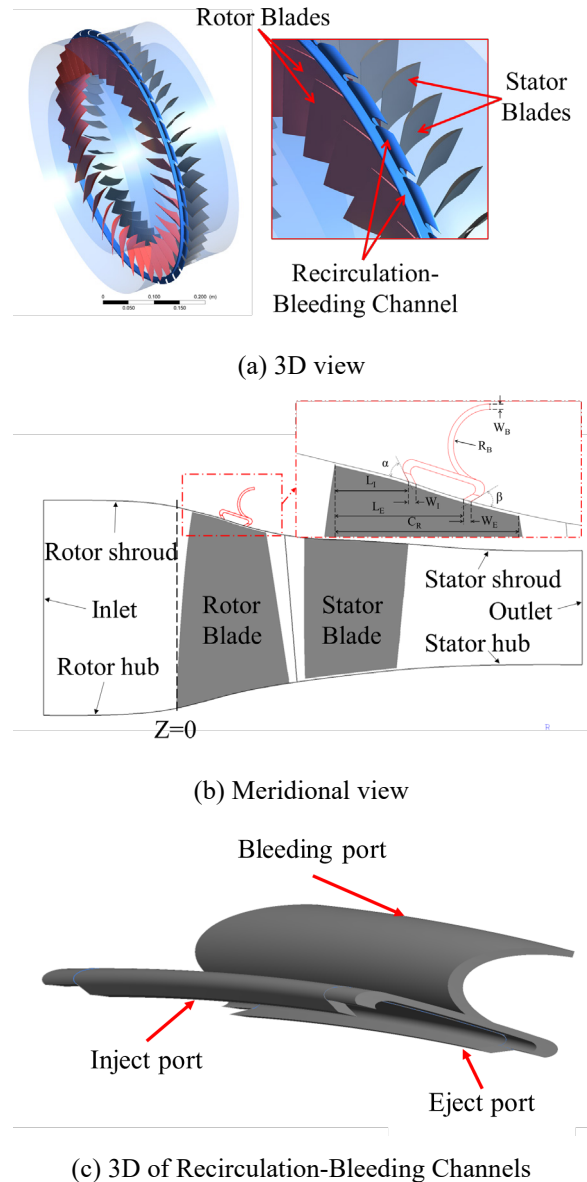


Fig. 1 Description of Recirculation-Bleeding channels

Based on the recirculation channel design [7], the angles (α and β) indicated the angles of injection and ejection, and the references of these angles are commonly 45° . The coverage angle (ϕ) indicated the angle of the annular coverage of the channel around the central axis in one rotor passage. Due to the need for mechanical support for the channel, the maximum value of this angle (reference value) was fixed at 8° . The locations of the injection and ejection ports for the recirculation channel (L_I , L_E) were measured from the rotor leading edge with the reference values of 40% and 70% of rotor tip chord length (C_R), respectively.

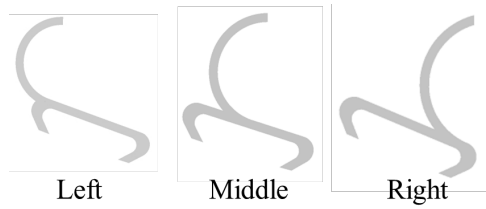


Fig. 2. Meridional positions of bleeding channels

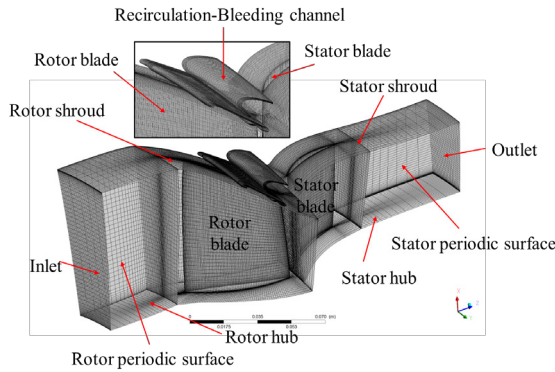


Fig. 3. Computational domains and grids

Three different locations of the bleeding channels along the upper surface of the recirculation channel, are presented at “Left”, “Middle” and “Right” as shown in Fig. 2.

2.2. Numerical method

The mesh of rotor and stator domains were used by Turbo-Grid®, whereas the computational domain of recirculation-bleeding channels was created using ICFM-CFD®, illustrated in Fig. 3. For the aerodynamic analysis, 3-D Reynold-Averaged Navier-Stokes (RANS) equations were solved using ANSYS CFX 19.1. ANSYS CFX-Pre, CFX-Solver and CFX-Post were used to define boundary conditions, solve the governing equations and postprocess the results, respectively. The working fluid is considered to be ideal air. Turbulence model $k-\varepsilon$ was used with scalable wall function with y^+ value ranging from 20 to 100.

The performance parameters of a single-stage transonic axial compressor, NASA stage 37 in this research were the total pressure ratio (PR), adiabatic efficiency (η), stall margin (SM), which were presented by Dinh et al. [7]:

$$PR = \frac{P_{t,out}}{P_{t,in}}$$

$$\eta = \frac{\left(\frac{P_{t,out}}{P_{t,in}}\right)^{\frac{\gamma-1}{\gamma}} - 1}{\left(\frac{T_{t,out}}{T_{t,in}}\right) - 1}$$

$$SM = \left(\frac{\dot{m}_{peak}}{\dot{m}_{stall}} \times \frac{PR_{stall}}{PR_{peak}} - 1 \right) \times 100\%$$

3. Results and discussion

Dinh et al. [7] presented the validation of a single-stage transonic axial compressor, NASA Stage 37 with the smooth casing optimum grid system of 590,080 nodes (Mesh 2) as shown in Fig. 4. Fig. 5 shows that the numerical and experimental results were good coincide, where the predicted peak adiabatic efficiency and stall margin, 83.85% and 9.95% are very close to the measurement, 84.00% and 10%, respectively.

Table 1 summarizes the numerical results of this investigation (Recirculation-bleeding channels) on aerodynamic performance of NASA Stage 37. It is clear that the recirculation-bleeding channels have positive effects on the aerodynamic performance of the single-stage compressor, where the total pressure ratio at the near-stall condition for all case of recirculation-bleeding channels is superior to that of smooth casing, except the stall margin for the “Middle” location of bleeding channels. The maximal value of total pressure ratio at the near-stall and peak conditions are 2.0976 and 2.0089, respectively, for “Middle” location of bleeding channels. The maximal efficiency value is 84.10% for “Left” location of bleeding channels. The value of 12.08 is the maximal stall margin with the “Right” location of bleeding channels in NASA Stage 37.

The existence of low-speed zones is a factor that degrade the performance of a compressor. Fig. 6 indicates that the size of low-speed zones was reduced with the application of recirculation-bleeding channels as compared to the smooth casing.

Another factor that contributes to the extension of stall margin is the spanwise length of reattachment and separation lines on rotor blades suction surface. Fig. 7 shows that these lines are pushed down away from blade’s tip, which helps prevent the stall inception. Nevertheless, the level of impact is different among the locations of bleeding channels. In the case of smooth casing, the separation line is located at about the rotor blade tip while the reattachment line is at approximately 85% of rotor blade span. The “Right” location of bleeding channels is the most effective on the separation and reattachment lines, about 93% and 76% of rotor blade span, respectively. With “Left” location of bleeding channels, while the spanwise length of reattachment line is highly reduced to 75 % of rotor blade span, the separation line was very close to the rotor tip, at about 98% of blade span.

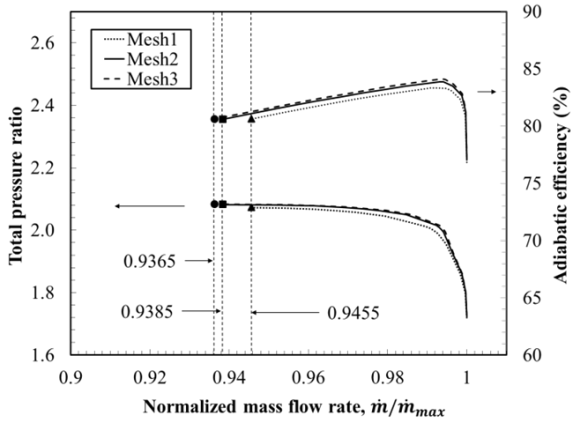


Fig. 4. Grid dependency tests for single-stage compressor, NASA stage 37

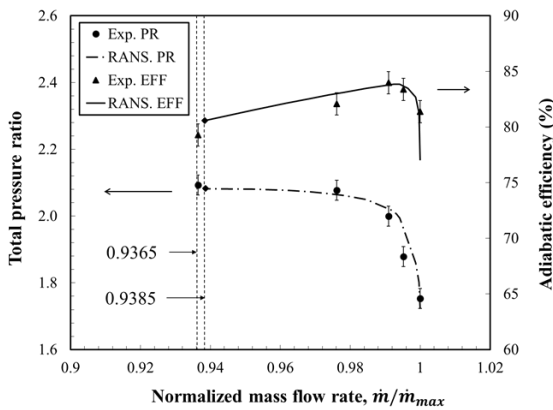


Fig. 5. Validation of numerical results with experimental data for NASA stage 37

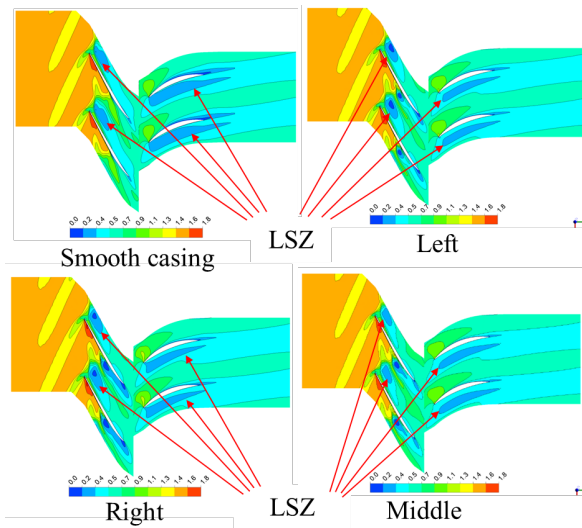


Fig. 6. Relative Mach number contour at 98% span at peak adiabatic efficiency condition

Table 1. Effects of recirculation-bleeding channels on aerodynamic performances of NASA Stage 37

Location	PR _{stall}	PR _{peak}	η (%)	SM (%)
SC	2.0802	2.0045	83.85	9.95
Left	2.0934	2.0076	84.10	11.36
Middle	2.0976	2.0089	84.06	9.85
Right (Ref.)	2.0868	2.0074	84.06	12.08

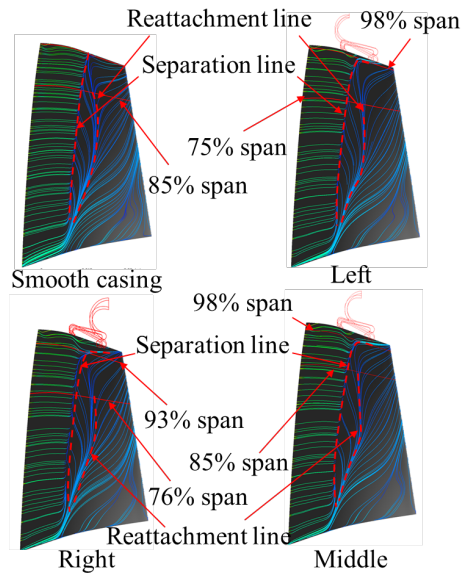


Fig. 7. Streamlines of reattachment and separation flow on rotor blade surface at near-stall condition

4. Conclusion

The study focuses on the enhancement ability of a new recirculation casing treatment, called recirculation-bleeding channels. These channels were investigated numerically to examine its effects on enhancing the aerodynamic performance of the single-stage transonic axial compressor, NASA Stage 37. These channels are capable of increasing the compressor's stall margin without any penalty in terms of adiabatic efficiency and pressure ratio. A reference design of the channels increased the stall margin by 21.43% with small improvement in peak adiabatic efficiency, by 0.25%. The location of the bleeding channels play an important role in the effectiveness of the recirculation-bleeding channels on the aerodynamic performance of the single-stage transonic compressor, NASA Stage 37.

Clearly, the study has not found the optimum design for this recirculation-bleeding channels. However, this preliminary investigation has shown positive result on the aerodynamic performance of this casing treatment. Further work is clearly

necessary to find the optimal design to maximize the aerodynamic performance of a single-stage transonic axial compressor.

Acknowledgments

This study is funded by the Vietnam National Foundation for Science and Technology Development under grant number 107.03-2018.20.

References

- [1] Hunter, I. H., and Cumpsty, N. A., 1982, Casing Wall Boundary-Layer Development Through an Isolated Compressor Rotor, *ASME Journal of Engineering for Power*, Vol 104(4), pp 805-817.
- [2] Koff, S. G., Mazzawy, R. S., Nikkanen, J. P., and Nolcheff, N. A., 1994, Case Treatment for Compressor Blades, U.S. Patent (5,282,718).
- [3] Hobbs, D. E., 1995, Active Vaned Passage Casing Treatment, U.S. Patent (5,431,533).
- [4] Nolcheff, N. A., 1996, Flow Aligned Plenum Endwall Treatment for Compressor Blades, U.S. Patent (5,586,859).
- [5] Hathaway, M. D., 2002, Self-Recirculating Casing Treatment Concept for Enhanced Compressor Performance, In *Proceedings of ASME Turbo Expo 2002*, Amsterdam, Netherlands, GT-2002-30368.
- [6] Strazisar, A. J., Bright, M. M., Thorp, S., Culley, D. E., and Suder K. L., 2004, Compressor Stall Control Through Endwall Recirculation, In *Proceeding of ASME Turbo Expo 2004*, Vienna, Austria, GT2004-54295.
- [7] Dinh, C. T., Ma, S. B., and Kim, K. Y., 2017, Effects of a Circumferential Feed-Back Channel on Aerodynamic Performance of a Single-Stage Transonic Axial Compressor, In *Proceedings of ASME Turbo Expo 2017: Turbomachinery Technical Conference and Exposition*, GT2017-63536.
- [8] Reid, L., and Moore, R. D., 1987, Design and Overall Performance of Four Highly Loaded, High-Speed Inlet Stages for an Advanced High-Pressure_Ratio Core Compressor, *NASA Technical Paper 1337*, Lewis Research Center, Cleveland, Ohio 44135.
- [9] ANSYS CFX-19.1, 2018, ANSYS Inc.,